J. Fluid Mech. (2013), *vol.* 724, *pp.* 695–703. © Cambridge University Press 2013
doi:10.1017/jfm.2013.183

A note on relative equilibria in a rotating shallow water layer

Hamid Ait Abderrahmane[1,†], Mohamed Fayed[2], Hoi Dick Ng[3] and Georgios H. Vatistas[3]

[1]Division of Mathematical and Computer Sciences and Engineering, King Abdullah University of Science and Technology (KAUST), Thuwal, Saudi Arabia

[2]Department of Mechanical Engineering, Alexandria University, Egypt

[3]Department of Mechanical and Industrial Engineering, Concordia University, Montreal, Quebec, Canada H3G 1M8

(Received 18 November 2012; revised 2 February 2013; accepted 8 April 2013; first published online 8 May 2013)

Relative equilibria of two and three satellite vortices in a rotating shallow water layer have been recorded via particle image velocimetry (PIV) and their autorotation speed was estimated. This study shows that these equilibria retain the fundamental characteristics of Kelvin's equilibria, and could be adequately described by the classical idealized point vortex theory. The same conclusion can also be inferred using the experimental dataset of Bergmann *et al.* (*J. Fluid Mech.*, vol. 679, 2011, pp. 415–431; *J. Fluid Mech.*, vol. 691, 2012, pp. 605–606) if the assigned field's contribution to pattern rotation is included.

Key words: vortex flows

1. Introduction

The idea of rotating N-point vortices was first used by Thomson (1878) (Lord Kelvin) as a basis to build the well-known (but now abandoned) vortex atom theory. Kelvin's conceptual polygons resemble closely those that which Mayer (1878) and Grzybowski, Stone & Whitesides (2000) observed in experiments with magnetized needles and millimetre-sized magnetized discs under the influence of an externally applied magnetic field. The point vortex model survived the decline of vortex atom theory and found applications in several fields of physics such as superfluidity, plasma physics and climatology; see Morikawa & Swenson (1971), Bauer & Morikawa (1976), Yarmuchk, Gordon & Packard (1979), Fine *et al.* (1995) and Durkin & Fajans (2000).

The question of linear stability of N equal strength vortices, positioned at the vertices of regular polygons, remains of particular interest for its theoretical and practical significance. This question was first tackled by Thomson (1883). A complete analysis of the stability of point vortices system including the influence of an assigned rotating background fluid (of relevance here) was carried by Havelock (1931). Recently, this linear stability analysis was generalized to the case of N helical vortices by Okulov (2004). Stable stationary vortex patterns are ubiquitous in rotating fluids. Examples include the vortex patterning observed in rotating superfluid ^{4} He, gyrating

† Email address for correspondence: haitabd@hotmail.com

https://doi.org/10.1017/jfm.2013.183 Published online by Cambridge University Press

electron columns confined in a Malmberg–Penning trap and stable helical multiplets of vortex in a rotating cavity flow; see Yarmuchk *et al.* (1979), Fine *et al.* (1995), Durkin & Fajans (2000) and Sørensen, Naumov & Okulov (2011).

Recently, using particle image velocimetry (PIV), Bergmann *et al.* (2011) reported experimental details on vortex patterns within a swirling shallow water layer. They have observed an ensemble of three satellite vortices, equally distributed in a ring of certain radius rotating around the axis of rotation in unison. The study by Bergmann *et al.* (2011), among other things, tried to verify the conjecture of Vatistas, Ait Abderrahmane & Siddiqui (2008) on the origin of the polygonal patterns in a hollow-core vortex within a swirling shallow water layer; see Vatistas (1990), Jansson *et al.* (2006) and Ait Abderrahmane, Siddiqui & Vatistas (2009) and Ait Abderrahmane *et al.* (2011). The conjecture was based on two strong observations and states that these polygons are the result of strong satellite vortices at their apexes. The first observation was the striking correspondence between the stability properties of these polygonal patterns and Thomson's point vortex configurations. The second was that the vortex ring to tank (boundary) radii ratios satisfied readily Havelock's (1931) limiting values for stability. The conclusion of Bergmann *et al.* (2011) was that these polygonal figures could not possibly be described by the simplified point vortex model.

The validity of the conjecture in Vatistas *et al.* (2008) is the central question examined also in the present paper. With respect to this question the results of Bergmann *et al.* (2011) as indicated in Bergmann *et al.* (2012) are inconclusive. The last is the result of not accounting for the background fluid rotation. Here by background flow we mean the flow inside the vortex ring induced by the rotating disc at the bottom of the container, which is characterized by more or less constant rotational speed (vorticity); see Bergmann *et al.* (2011, figure 7(*c*)) and Bergmann *et al.* (2012, figure 1(*b*)), respectively. It will be confirmed below that the background flow inside the ring is in solid-body-like rotation. Although an accurate way to estimate the background flow could be a matter of discussion, such flow cannot be simply omitted when the question arises of whether or not the observed regular vortex pattern can be described by the old point vortex theory, so we address this here.

The flow under consideration is complex but by employing the experimental approach of Bergmann *et al.* (2011), one can gain a deeper insight of the event. In order to acquire additional details of the phenomenon, we carefully conducted our experiments, following a similar experimental method as in Bergmann *et al.* (2011). We show that our results and in fact those presented in Bergmann *et al.* (2011, 2012) support the fact that the flow under consideration can be reasonably described by the point-vortex theory if the contribution of the assigned flow is taken into consideration. In order to estimate the rotational speed of the vortex pattern, Bergmann *et al.* (2011, 2012) as well as the present work require a formula that accounts for the background fluid rotation, see Havelock (1931). The relationship employed by Bergmann *et al.* (2011, 2012) (their equation (4.1)) is only applicable to the case of a quiescent carrier fluid, or in the frame of reference rotating with the bulk fluid, inside the vortex ring. We show here that accounting for the last detail, our present experiments and indeed those of Bergmann *et al.* (2011) indicate that the measured speed of pattern autorotation is consistent with that predicted by the idealized point vortex theory.

https://doi.org/10.1017/jfm.2013.183 Published online by Cambridge University Press

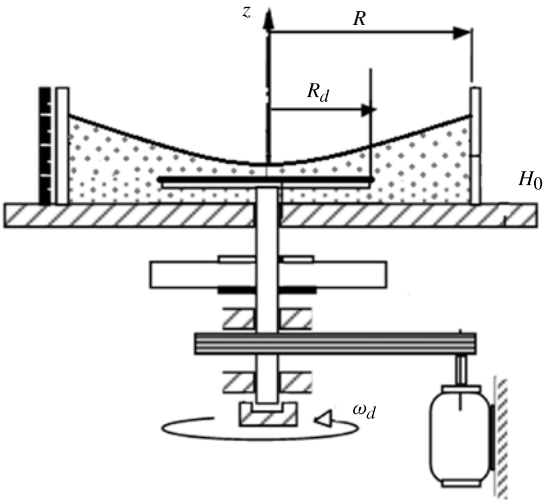


FIGURE 1. A schematic of the experimental apparatus. The present tests were conducted using tap water. The height of the (quiescent) water layer H_0 was 34 and 40 mm, the disc and tank radius were $R_d = 126$ mm and $R = 142$ mm, respectively.

2. Experiment set-up

The experimental set-up employed in this study is the same as that described in more detail in Vatistas *et al.* (2008). A shallow layer of water was brought into swirl by a rotating disc (in the counterclockwise direction) at the bottom of a Plexiglas stationary cylindrical tank; see figure 1. The main control parameter is the frequency f of the rotating disc. The height H_0 of the (quiescent) water layer, the radius R and R_d of the cylindrical container and the disc could also be considered as other control parameters but in our experiments these were kept constant. The flow field on the free surface of the swirling shallow water layer was obtained using PIV. White Polystyrene 250 μmm spherical particles (lighter than water), spread as sparsely as possible over the free surface, were used to measure the velocity field at the free surface. The flow field dynamics are imaged from above using a high-speed camera (model PCO.1200 hs). A sample of raw images used for the data analysis are shown in figure 2(*a,b*).

The data analysis began with the extraction of the flow field on the free liquid surface as viewed by an observer located in the laboratory frame of reference. The streamlines for this flow field, shown in blue in figure 3(*a,b*), were constructed first. The streamlines of the combined flow as seen by an observer rotating with the background fluid are illustrated in figure 3(*a,b*). This is achieved by subtracting the counterclockwise background flow, which as shown below rotates at a constant angular velocity. In this frame of reference, a central vortex (in green) comes into view. For the case of a two-vortex pattern, the central vortex is absent, perhaps because it was too weak to be observed. Counterclockwise-rotating satellite vortices (in black) and clockwise rotating lateral vortices (in red) are nested into the background flow. The latter are located outside the vortex ring at the disc radius, R_d, and they are similar to those following the shear layer instability in rotating fluid, see Rabaud & Couder (1983) and Poncet & Chauve (2007). Note that the interplay between the inertial and

https://doi.org/10.1017/jfm.2013.183 Published online by Cambridge University Press

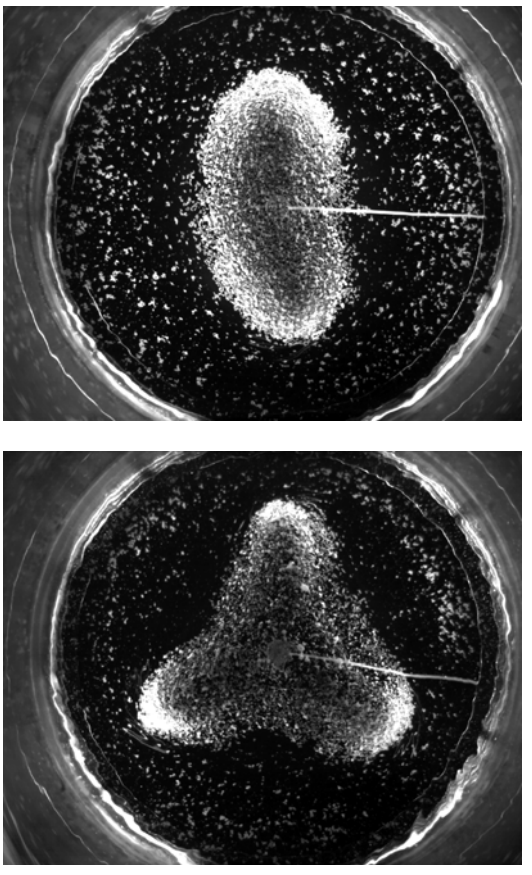


FIGURE 2. Sample of raw images used in the data analysis showing the white Polystyrene particles that were distributed on the free surface.

shear instabilities or between the vortices inside and outside the vortex ring can be an interesting research that is beyond the scope of the present paper.

In the frame of the present study that is limited to counterclockwise-rotating satellite vortices, the lateral vortices seem not to have a significant influence. The counterclockwise-rotating satellite vortices are arranged symmetrically on a ring around the axis of rotation. These, having swirling speeds that are higher than the carrier fluid ($\cong$3 times more in the case of triangular pattern and $\cong$2 times more in the case of an ellipsoidal pattern) distort the otherwise circular streamlines of the underlying flow thus giving them a polygonal shape. A schematic of the flow configuration is displayed in figure 4(*a*). Here, the rotating background fluid speed was estimated using the flow velocity measured along a ray that begins at the origin and passes through a satellite vortex. Along this ray the influence of the central, satellite and lateral vortices which are expected to modulate the motion of the assigned swirling flow field is minimal. Also along this ray the water depth is low enough to match the one assigned by the rotating disc. The flow measurements indicate that the background fluid motion is in solid-body rotation; see figure 5. This corresponds to the quasi-straight dotted-line of figure 7(*c*) in Bergmann *et al.* (2011) and more or less to a constant vorticity plateau inside the vortex ring, see figure 1(*b*) in Bergmann *et al.*

https://doi.org/10.1017/jfm.2013.183 Published online by Cambridge University Press

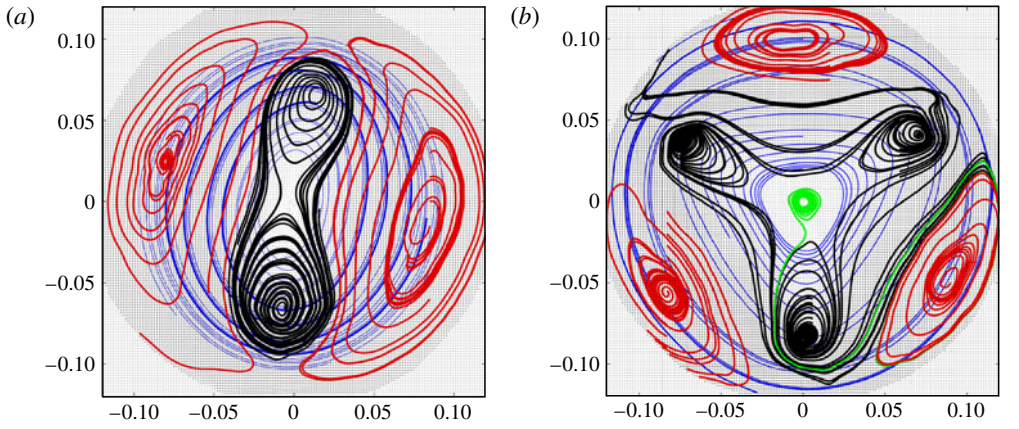


FIGURE 3. Streamline configuration constructed based on the surface flow PIV measurements. The blue lines indicate the streamlines of the flow field as seen from the laboratory frame of reference. The black lines represent the streamlines as seen by an observer rotating with the fluid angular velocity $\Omega(R_v)$, where R_v (ring radius; where the centres of the satellite vortices are located). The green line represents the central vortex while the red lines represent the clockwise-rotating lateral vortices.

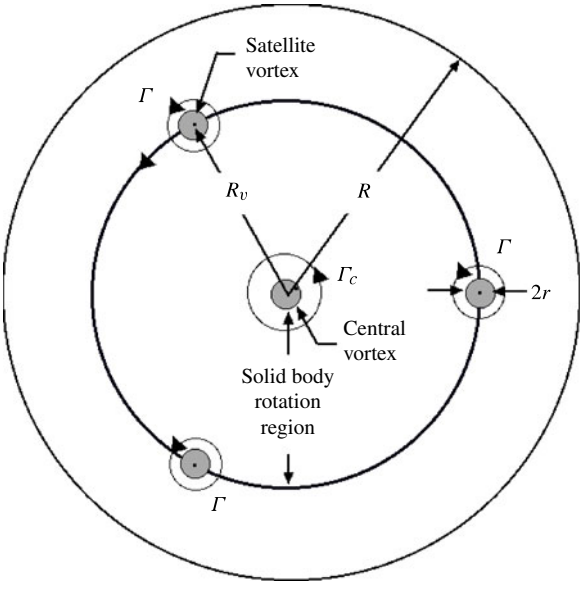


FIGURE 4. Schematic of the satellite vortices distribution.

(2012). Here, we would like to point out that the highly spiky vorticity plateau inside the vortex ring is unphysical; this should stem from the order of approximation of the derivative used in the calculation of their vorticity from the velocity field. In this case working with the velocity field, as done in our study, shall provide more confidence than working with vorticity.

https://doi.org/10.1017/jfm.2013.183 Published online by Cambridge University Press

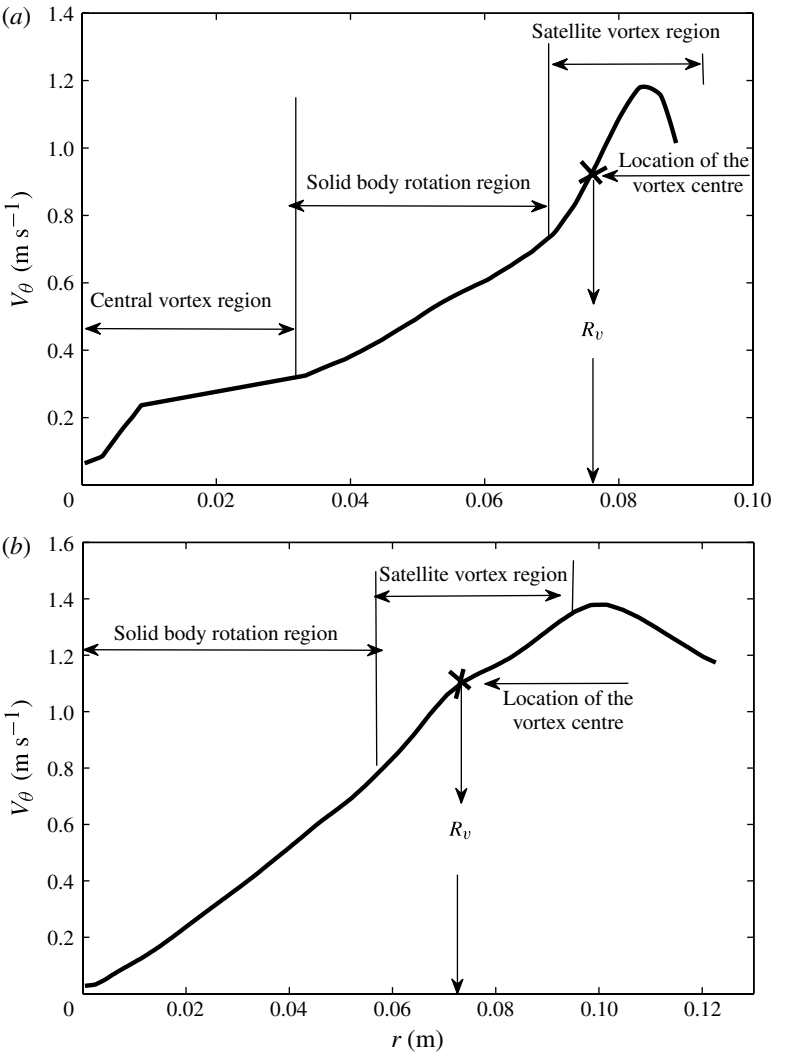


FIGURE 5. Tangential velocity V_θ in the laboratory frame of reference as function of distance (in metres) from the rotation axis on a ray passing through a satellite vortex: (*a*) triangular pattern; (*b*) ellipsoidal pattern.

3. Results and discussion

The kinematics of these vortex ensembles in relation to the background flow can be described by the relation provided by Havelock (1931) for a system of vortices arranged in ring in an assigned flow, i.e.

$$\Omega\,(R_v)_p\,/_l = \frac{(N-1)\Gamma}{4\pi R_v^2} + \Omega\,(R_v)_f\,/_l, \tag{3.1}$$

where $(N-1)\Gamma/4\pi R_v^2$ is the autorotation of the vortex system for an observer rotating with angular speed of the assigned flow, and $\Omega(R_v)$ and Γ are the angular velocity of the ring (of radius R_v) and the circulation of a satellite vortex, respectively. The

https://doi.org/10.1017/jfm.2013.183 Published online by Cambridge University Press

subscripts p, f and l indicate vortex pattern, fluid and laboratory, respectively, while / denotes 'relative to'.

In the case of the system of three vortices, the angular velocity of the background flow, i.e. the slope of the solid-body rotation region, is found to be 10.8 rad s^{-1}, see figure 5(a). The strength or the circulation Γ of the satellite vortices in (3.1) is estimated as $2\pi rv$, where $r = 10$ mm and $v = V_\theta(R_v + r) - V_\theta(R_v) = 0.33$ m s^{-1} where r denotes the radius of the satellite vortex, v the tangential velocity relative to the background flow and $R_v = 0.075$ m. The estimated autorotation of the vortex system is 0.6 rad s^{-1} and hence the angular velocity of the pattern estimated from (3.1) is 11.4 rad s^{-1}. However, the measured value from the recorded raw images is 11.9 rad s^{-1}. The difference between the estimated and the measured values of the angular velocity of the three-vortex ensemble is approximately 4 %. According to Havelock (1931) the autorotation of the vortex arrangement with outer boundary is

$$\frac{(N-1)\Gamma}{4\pi R_v^2} + \frac{\Gamma}{2\pi R_v}\sum_{s=0}^{N-1}\frac{(R^2/R_v)C - R_v}{R^4/R_v^2 + R_v^2 - 2R^2C} \tag{3.2}$$

where $C = \cos(2s\pi/N)$. Therefore, the difference becomes approximately 3 % if one considers the influence of the cylindrical boundary.

Similar analysis was also carried out on a system of two satellite vortices, see figure 5(b). The angular velocity of the background flow is found to be 13.4 rad s^{-1}, see figure 5(b). The estimated autorotation of the vortex system is 0.5 rad s^{-1} and, hence, the angular velocity of the pattern estimated from (3.1) is 13.9 rad s^{-1}. However, the measured autorotation of the vortex system from the recorded raw images is 14.9 rad s^{-1}. The difference between the estimated and the measured values of the angular velocity of the three-vortex ensemble is approximately 7 %. Based on the above analysis, one can easily see that in order to compare the angular velocities in the laboratory frame of reference, equation (4.1) of Bergmann *et al.* (2011, 2012) should have included the contribution of the assigned flow field, as shown by Havelock (1931). In the following we demonstrate that if Bergmann *et al.* (2011) had taken into consideration the rotation of the carrier fluid, then the estimated and measured angular velocities in the laboratory frame of reference would not differ by one order of magnitude.

The first issue that one can easily note in Bergmann *et al.* (2011) is the estimation of the rotational angular speed of the vortex pattern. The given value of 2.44 rad s^{-1}, considered as the angular speed of the pattern, is in fact the rotational speed of the quasi-solid-body rotation of the background flow $\Omega\,(R_v)_f\,/_l$ as defined previously. Otherwise, one could not justify or explain the fact that vortices at each arm can still be observed after subtracting the rotation rate of the figure, see figure 8(b) in Bergmann *et al.* (2011). The vortices were observable because the background flow and not the rotation rate of the figure has been subtracted. However, if one uses the flow measurements to estimate the angular speed of the pattern, then the angular velocity of the vortex centres or vortex ring located at radius ($R_v \approx 110$ mm) from the centre of the rotation provide a more appropriate value for the speed of the ensemble. The last angular velocity value can be obtained from the curve represented in figure 7 of Bergmann *et al.* (2011) by a dotted line; its value is $V_\theta\,(R_v)_p\,/_l = 302$ mm s^{-1}. Hence, the speed of the vortex pattern is $\Omega\,(R_v)_p\,/_l = 302/110 = 2.74$ rad s^{-1}. As expected, this value is higher than that of the fluid (2.44 rad s^{-1}), which also explains the spiralling effects around the satellite vortices as also mentioned by Bergmann *et al.* (2011). Owing to mutual advection,

https://doi.org/10.1017/jfm.2013.183 Published online by Cambridge University Press

the angular speed of the vortex pattern is the difference between the rotational speed of the ensemble and the background flow; both estimated in the laboratory frame of reference, i.e. $\Omega\,(R_v)_p\,/_l - \Omega\,(R_v)_f\,/_l = \Omega\,(R_v)_p\,/_f = 2.74 - 2.44 = 0.3$ rad s^{-1}. The last value is very close to the estimated value (0.26 rad s^{-1}) obtained using equation (4.1) of Bergmann *et al.* (2011, 2012).

The same result can also be obtained via the additional data provided in figure 1(*b*) of Bergmann *et al.* (2012). Their figure indicates that the maximum total vorticity value (satellite vortex plus background fluid) is approximately $\Omega_{total} = 20$ rad s^{-1}, and that the average vorticity in the region inside the ring is $\Omega_{fluid} \approx 6$ rad s^{-1}. Hence, for an observer in the rotating frame of reference riding the background flow, the vorticity inside the satellite vortices is $\Omega_{vortex} = \Omega_{total} - \Omega_{fluid} = 14$ rad s^{-1}. The rotational speed of a satellite vortex is then $\omega = \Omega_{vortex}/2 = 7$ rad s^{-1}. The maximum tangential velocity of the vortex can be calculated as $V = \omega r = 0.14$ m s^{-1} provided that the radius of this vortex $r = 0.020$ m. Hence, using (4.1) in Bergmann *et al.* (2011) the rotational speed of the three-vortex system in the fluid frame of reference is $\Omega_{fluid} = Vr/R_v^2 = 0.23$ rad s^{-1} (where $R_v = 0.110$ m is the radius of the vortex ring). This value is very close to the value (0.26 rad s^{-1}) given by Bergmann *et al.* (2011, 2012). Note that this estimation can essentially vary due the uncertainty in the evaluation of the average vorticity inside the vortex ring because of the spiky profile.

4. Conclusion

The present work fortifies our previous conjecture in Vatistas *et al.* (2008) that the observed regular vortex patterns are a real fluid manifestation of the venerable fluid flow problem, idealized long ago via Hamiltonian potential point vortices. The strengthening of our original argument involves the value of the pattern speed which is shown to be consistent with that predicted using the old simplified theory by Havelock (1931). Additional evidence in support of the present confirmation is the fact that stability conditions of this cluster, in terms of the ratio R_v/R (where R is the radius of the containing vessel), are very close to Havelock's theoretical limits 0.567 and 0.462 for three- and two-vortex patterns, respectively. The corresponding ratios found experimentally are $R_v/R = 0.53$ and $R_v/R = 0.49$ for three- and two-vortex ensembles, respectively. The same holds true for the case of Bergmann *et al.* (2011) where their experimental data yielded a ratio of 0.567.

REFERENCES

Ait Abderrahmane, H., Siddiqui, K., Vatistas, G. H., Fayed, M. & Ng, H. D. 2011 Symmetrization of polygonal hollow-core vortex through beat-wave resonance. *Phys. Rev.* E **83**, 056319.

Ait Abderrahmane, H., Siddiqui, K. & Vatistas, G. H. 2011 Rotating waves within a hollow vortex core. *Exp. Fluids* **50**, 677–688.

Ait Abderrahmane, H., Siddiqui, K. & Vatistas, G. H. 2009 The transition between Kelvin's equilibria. *Phys. Rev.* E **80**, 066305.

Bauer, L. & Morikawa, G. K. 1976 Stability of rectilinear geostrophic vortices in stationary equilibrium. *Phys. Fluids* **19**, 929–942.

Bergmann, R., Tophøj, L., Homan, T. A. M., Hersen, P., Andersen, A. & Bohr, T. 2011 Polygon formation and surface flow on a rotating fluid surface. *J. Fluid Mech.* **679**, 415–431.

Bergmann, R., Tophøj, L., Homan, T. A. M., Hersen, P., Andersen, A. & Bohr, T. 2012 Erratum: polygon formation and surface flow on a rotating fluid surface. *J. Fluid Mech.* **691**, 605–606.

https://doi.org/10.1017/jfm.2013.183 Published online by Cambridge University Press

DURKIN, D. & FAJANS, J. 2000 Experiments on two-dimensional vortex patterns. *Phys. Fluids* **12**, 289–293.

FINE, K., CASS, A., FLYNN, W. & DRISCOLL, C. 1995 Relaxation of 2D turbulence to vortex crystals. *Phys. Rev. Lett.* **75**, 3277–3280.

GRZYBOWSKI, B. A., STONE, H. A. & WHITESIDES, G. M. 2000 Dynamic self-assembly of magnetized, millimetre-sized objects rotating at a liquid–air interface. *Nature* **405**, 1033–1036.

HAVELOCK, T. H. 1931 The stability of motion of rectilinear vortices in ring formation. *Philos. Mag.* **11**, 617–633.

JANSSON, T. R. N., HASPANG, M. P., JENSEN, K. H., HERSEN, P. & BOHR, T. 2006 Polygons on a rotating fluid surface. *Phys. Rev. Lett.* **96**, 174502.

MAYER, A. M. 1878 Experiments with floating magnets. *Nature* **17**, 487–488.

MORIKAWA, G. K. & SWENSON, E. V. 1971 Interacting motion of rectilinear geostrophic vortices. *Phys. Fluids* **14**, 1058–1071.

OKULOV, V. L. 2004 On the stability of multiple helical vortices. *J. Fluid Mech.* **521**, 319–342.

PONCET, S. & CHAUVE, M. P. 2007 Shear-layer instability in a rotating system. *J. Flow Visual. Image Process.* **14**, 85–105.

RABAUD, M. & COUDER, Y. 1983 A shear-flow instability in a circular geometry. *J. Fluid Mech.* **136**, 291–319.

SØRENSEN, J. N., NAUMOV, I. V. & OKULOV, V. L. 2011 Multiple helical modes of vortex breakdown. *J. Fluid Mech.* **683**, 430–441.

THOMSON, J. J. 1883 *A Treatise on the Motion of Vortex Rings*. Macmillan & Co.

THOMSON, W. (LORD KELVIN) 1878 Floating magnets. *Nature* **18**, 13–14.

VATISTAS, G. H. 1990 A note on liquid vortex sloshing and Kelvin's equilibria. *J. Fluid Mech.* **217**, 241–248.

VATISTAS, G. H., AIT ABDERRAHMANE, H. & SIDDIQUI, K. 2008 Experimental confirmation of Kelvin's equilibria. *Phys. Rev. Lett.* **100**, 174503.

YARMUCHK, E., GORDON, M. & PACKARD, R. 1979 Observation of stationary vortex array in rotating superfluid helium. *Phys. Rev. Lett.* **43**, 214–217.

https://doi.org/10.1017/jfm.2013.183 Published online by Cambridge University Press